UC Category: 60

NASA Conference Publication 2230
DOE Publication CONF-810752
SERI/CP-635-1273

Large Horizontal-Axis Wind Turbines

Robert W. Thresher, Editor
Oregon State University
Corvallis, Oregon

Proceedings of a workshop sponsored by
U. S. Department of Energy
Wind Energy Technology Division, and
NASA Lewis Research Center and held in
Cleveland, Ohio
July 28-30, 1981

National Aeronautics
and Space Administration

Scientific and Technical
Information Branch

1982

PERFORMANCE AND LOAD DATA FROM MOD-OA AND MOD-1 WIND TURBINE GENERATORS

David A. Spera and David C. Janetzke
National Aeronautics and Space Administration
Lewis Research Center
Cleveland, Ohio

ABSTRACT

Experimental data, together with supporting analysis, are presented on the power conversion performance and blade loading of large, horizontal-axis wind turbines tested at electric utility sites in the U.S. Four turbine rotor configurations, from 28 to 61 meters in diameter, and data from five test sites are included. Performance data are presented in the form of graphs of power and system efficiency versus free-stream wind speed. Deviations from theoretical performance are analyzed statistically. Power conversion efficiency averaged 0.34 for all tests combined, compared with 0.31 predicted. Round blade tips appeared to improve performance significantly. Cyclic blade loads were normalized to develop load factors which can be used in the design of rotors with rigid hubs.

INTRODUCTION

This paper presents experimental data and supporting analysis of the power conversion performance and blade loading of large, horizontal-axis wind turbines tested at electric utility sites in the U.S. These tests were conducted by the National Aeronautics and Space Administration (NASA) as part of the federal wind energy program administered by the Department of Energy (DOE). The principal objectives of this work are (1) to provide performance and load test data for wind turbine design, (2) to evaluate the PROP-L2 computer program for predicting the efficiency of propeller-type wind turbines, and (3) to examine a proposed energy method for testing wind turbine system performance.

Data from tests of four turbine rotor configurations are analyzed in this paper. The airfoil shapes and dimensions of each configuration are listed in Table I, and their planforms are illustrated in Figure 1. The rotors studied had two blades each and ranged in diameter from 28 to 61 meters. Thickness-to-chord ratios at 75 percent of span varied from 0.156 to 0.240. Two NACA airfoils and four skin materials were tested. One configuration had semi-circular blade tips. Blades in the other three configurations had square tips.

As shown in Table II, test data have been grouped according to the configuration of the rotor and the turbine shaft speed into six test series. Each of these series is a combination of several data records, one to six hours long, which were selected to represent a variety of operating conditions.

Data on test installations are also given in Table II. Rotor configurations 1, 2, and 3 were tested on Mod-0A machines, while configuration 4 was tested on the larger Mod-1 system (ref. 1). These experimental wind turbines are of the "first generation" type (ref. 2), with the following design characteristics in common: Two blades, fully pitchable for power control; rotor hub rigidly attached to the turbine shaft; turbine rotor located downwind of a stiff truss tower; parallel-axis gearbox with a single speed ratio; synchronous AC generator; and active yaw control.

Preliminary performance and load data measured on the Mod-0A and Mod-1 systems were presented in References 3 to 8. The data contained in this paper significantly extend those reported earlier, by including additional rotor configurations and wind turbine test installations, moderately long operating periods and additional statistical analysis. Therefore, the performance and load data presented here can be regarded as typical of the first generation of large, horizontal-axis wind turbines.

PROCEDURE

Test Installation and Data

Details of the DOE/NASA wind turbine test installations, instrumentation, and data acquisition system have been presented previously (ref. 9 and 10, for example), so only a brief discussion will be given here. Figure 2 illustrates the test installation at Clayton, New Mexico, which is typical of all the installations listed in Table II. At each test site, an auxiliary anemometer tower is located several rotor diameters from the turbine tower, in the direction of the prevailing wind. Signals from a variety of transducers located throughout the test system are recorded on analog tape, digitized, and then processed to produce statistical information and graphical displays. Data are recorded automatically during normal operation of the wind turbine generator as a powerplant on the electric utility system.

The four parameters of specific interest in this study of turbine performance and loads are as follows:

1. Free-stream wind speed at hub elevation, V_0, measured by an anemometer on the auxiliary tower at the elevation of the turbine axis (Station 0, fig. 2). Averaging time was selected as 30 seconds and the anemometer length constant was 1.5 meters. Wind data were purposely limited to measurements from a single anemometer, because one free-stream anemometer is often all that is available.

2. Output electrical power, P_3, measured at the generator terminals (Station 3, fig. 2).

3. Two components of cyclic bending load on the blade root, δM_y and δM_z. Cyclic load is a typical measure of fatigue loading and is calculated for each turbine revolution as follows:

Flatwise (out-of-plane): $$\delta M_{y,i} = 0.5(M_{y,max}-M_{y,min})_i \quad (1a)$$

and

Chordwise (in-plane): $$\delta M_{z,i} = 0.5(M_{z,max}-M_{z,min})_i \quad (1b)$$

in which i is the rotor revolution number and max and min designate the extreme values of the load measured during that revolution.

Theoretical Output Power

Theoretical turbine power, as a function of free-stream wind speed, was calculated by means of a modified version of the commonly-used PROP FORTRAN computer program (ref. 11), designated as PROP-L2. Recent tests on wind turbine rotors in the stalled condition (ref. 12) indicated the need for improved aerodynamic modeling in the basic PROP program. In the PROP-L2 version, aerodynamic losses at square tips are included within the blade-element algorithms by introducing the following two modifications:

1. Correcting reference lift and drag curves for planform aspect ratio (refs. 12 and 13).

2. Using "smooth" airfoil properties, instead of "rough" or "half-rough," as in previous studies (ref. 8, for example).

A comparable theory for the aerodynamic losses at rounded blade tips has not yet been developed. Therefore, test data for configuration 3R, with semi-circular tips, are compared with theoretical calculations for square-tipped blades, to identify differences which may be attributable to tip shape.

In addition to the PROP-L2 computer program for turbine power, a model for losses in the power train is required before generator output can be predicted. A general power-train loss model which was developed for this study is as follows:

$$P_{23} = P_3-P_2 = -aP_{3,r} -(b+s)P_2 \quad (2)$$

in which

P_{23} power-train loss, kW

P_2, P_3 turbine and generator output power, respectively, kW

$P_{3,r}$ rated output power, kW

a,b empirical constants

s slip ratio

For the Mod-0A power trains, a is 0.055, b is 0.040, and s is 0.025. For the Mod-1 system, a is 0.027, b is 0.059, and s is zero.

Energy Method for Evaluating Performance

The performance of the wind-turbine-generator system can be evaluated by measuring either its power conversion efficiency or its energy conversion efficiency. Previous studies have used power as the primary performance parameter, with energy (and particularly annual output energy) as a derived parameter. Data have generally been statistically analyzed by the "method of bins" (refs. 8 and 14). An alternative method has been developed for this study, in which energy is the primary parameter, power is a derived parameter, and the required amount of statistical analysis is greatly reduced or eliminated.

The energy method for evaluating the performance of wind turbine systems appears to offer advantages of simplicity and repeatibility, compared with the method of bins. Also, evaluation of theoretical methods for predicting performance may be more relevant to operation when comparisons are made on the basis of energy capture rather than instantaneous power. A committee of the American Society of Mechanical Engineers is now evaluating the energy method as a basis for a performance test code for wind turbine generators.

To apply the energy method, the following steps are performed:

1. Divide the test period into time increments, Δt. Each time increment should be 5 to 10 times as long as the longest wind transit time from the free-stream anemometer to the turbine (fig. 2). Time increments of this length reduce time correlation errors but still permit comparison of test data with steady-state theoretical power curves. In this study time increments were 10 minutes long.

2. During each time increment measure the time history of the free-stream wind speed at the turbine midline elevation, $v_o(t)$. Calculate the mean wind speed, V_o, the increment in wind energy flux, Δe_o, and the mean wind power flux, p_o, for each time increment, as follows:

$$V_o = \frac{1}{\Delta t}\int_{\Delta t} v_o(t)dt \quad , \qquad \text{m/s} \qquad (3a)$$

$$\Delta e_o = \frac{\rho}{2}\int_{\Delta t} [v_o(t)]^3 \, dt \quad , \qquad \text{W-s/m}^2 \qquad (3b)$$

and

$$p_o = \Delta e_o/\Delta t \quad , \qquad \text{W/m}^2 \qquad (3c)$$

3. For each time increment measure the corresponding increment in electrical output energy, ΔE_3. Calculate increments in output energy flux, Δe_3, mean output power, P_3, and the mean output power flux, p_3, as follows:

$$\Delta e_3 = \Delta E_3/A \quad , \qquad W\text{-}s/m^2 \qquad (4a)$$

$$P_3 = \Delta E_3/\Delta t \quad , \qquad W \qquad (4b)$$

and

$$p_3 = P_3/A \quad , \qquad W/m^2 \qquad (4c)$$

in which A is the area of the surface swept by the turbine rotor, as projected on a vertical plane.

4. For each time increment, calculate the system energy conversion efficiency, as follows:

$$\eta_3 = \Delta e_3/\Delta e_o = p_3/p_o \qquad (5)$$

5. Evaluate system performance by means of data from steps 2 to 4. Evaluation may be based on any or all of the following: (a) Power curves, such as P_3 and p_3 versus V_o, (b) efficiency curves, such as η_3 versus V_o, and (c) statistical analysis of deviations from available theory.

RESULTS AND DISCUSSION

Power Conversion Performance

Performance test results for each of the four rotor configurations described in Table I are presented in the following three formats:

First, Figures 3 to 6 show graphically the variation of output power and system efficiency with wind speed for each configuration. Secondly, summaries of test conditions, measured mean power and efficiency, and theoretical mean power and efficiency are listed in Table III. Finally, Table IV contains the results of a statistical analysis of deviations between the test data and theoretical performance.

The test series during which performance data were taken are those listed in Table II as series 1.1, 2.1, 3.1R, and 4.1. Only blade load data from test series 1.2 and 2.2 are included in this study. Performance test runs were selected to emphasize wind conditions below rated, for which efficiency data are most significant. However, no attempt was made to select periods of steady wind. Instead, the variability of the wind power source was included so that these data would be typical of automatic, unattended wind turbine operations in below-rated winds. In all cases, the

experimental wind turbine was the only wind power unit on the test site.

Figures 3 to 6 present comparisons between theoretical and experimental performance. The theoretical power curves are for "site standard" conditions, in which air density is equal to the U.S. Standard Atmosphere density for the site altitude. Test data were also adjusted to site standard conditions, with the exception of test series 2.1. Atmospheric pressure data were not available for this test series. Each data point represents average performance during a 10-minute period of operation under automatic control.

While some qualitative comparisons between theory and experiment can be made from these figures, the amount of scatter is such that statistical analysis is required. This scatter is typical of tests on large wind turbines and indicates that wind conditions over the turbine swept area and those sampled by the free-stream anemometer were not completely correlated. As expected, scatter of the efficiency data is greater than that of the power data, because wind speed correlation errors are amplified when the speed is cubed to calculate wind power flux.

Another commonly observed phenomenon is shown clearly in Figure 4(a) by the data at the transition from below-rated to above-rated wind speeds. Data in this region usually fall below the theoretical "corner", because average power is always lowered whenever the power control system is active. Nevertheless, inspection of Figures 3 to 6 indicate that (1) zero-power or cut-in wind speeds were predicted within 0.5 meter per second, (2) slopes of the theoretical power curves were in general agreement with the test data, (3) test data points for configuration 3R (the 14 meter wood/composite blades with semi-circular tips) almost always exceeded theoretical performance, and (4) test data verified the predicted highest efficiency of rotor configuration 4.

Table III summarizes the results of these four series of performance tests in quantitative terms. For example, test series 1.1 was composed of data records totaling 11 hours in length, with a mean wind speed of 7.7 meters per second, equivalent to a mean tip speed ratio of 10.5. During this period, the mean wind power flux at the turbine hub elevation was 270 Watts per square meter. Mean electrical output power flux was measured at 90 Watts per square meter. This indicates an average system efficiency of 0.33, the same as the theoretical value. Similarly, during test series 2.1, the mean power conversion efficiency was equal to the theoretical efficiency.

The semi-circular tips on the blades in configuration 3R appear to have increased the performance of these airfoils significantly, compared to predictions for the same blades with square tips. Based on the results of test series 1.1 and 2.1, the mean efficiency of rotor configuration 3 with square tips would not be expected to

exceed 0.26. However, with semi-circular tips this rotor configuration operated with a mean efficiency of 0.32. This indicates an improvement of more than 20 percent in energy production during operation below rated power. To verify this improvement, tests of configuration 3 blades with square tips are planned. This amount of improvement, however, may be limited to low aspect ratio blades. Further tests are required to evaluate the effects of tip shape on the performance of blades with higher aspect ratios.

If the results of all four series of performance tests are combined by weighted averaging into one data set as shown in the last line of Table III, this set would represent a sample of current experience with large, first-generation, propeller-type rotors. Including the effects of different tips and site roughnesses, an overall efficiency of 0.34 has been achieved in predominantly below-rated winds. This compares very well with a theoretical power conversion efficiency of 0.31 for the same wind conditions.

Statistical analysis of deviations between the performance test results and predictions made using the PROP-L2 computer program are summarized in Table IV. The mean deviation of the samples from the common base of the theory shows a performance advantage of more than 9 percent of rated power for configuration 3R over the composite performance of the three other configurations. This difference in performance has been attributed to the difference in tip shape although this has yet to be verified. Standard deviations for the four test series are remarkably consistent at 5 to 6 percent of rated power. This indicates that the scatter observed in Figures 3 to 6 is repeatable and acceptable for purposes of performance evaluation.

By analyzing deviations between test and theory, the theoretical power curve can be adjusted to serve as a lower bound on predicted performance. The size of the adjustment depends on the desired confidence in the predicted lower bound. Standard statistical analysis methods can be used to calculate the adjustment, as discussed in Reference 8. As shown in the last column of Table IV, if the predicted mean power flux of a rotor with square tips is reduced by 3 Watts per square meter, there is a 0.999 confidence level that the mean power during long-term tests will not be less than this reduced value. For blades like those of configuration 3R, with semi-circular tips, an <u>increase</u> in the theoretical power flux of 26 Watts per square meter is consistent with a 0.999 lower bound on mean performance. However, additional tests are required to support this latter conclusion.

To summarize the results of the performance testing in this study, the wind turbine generators converted about one-third of the incident wind energy to electricity, the PROP-L2 computer program was verified as a performance prediction method, and lower bounds on performance were estimated.

Blade Bending Load Data

Dynamic loads sustained by rotor blades on large, horizontal-axis wind turbines were measured during all six test series listed in Table II. The load data obtained are typical of first-generation wind turbines, which are characterized by rigid hubs, rotors located downwind of truss towers, and full-span pitch controls. Load test results are shown in Figures 7(a) to 7(d) in the form of cumulative probability distributions useful for fatigue life analysis. Cyclic flatwise and cyclic chordwise load components are given for each test series. Component directions are referred to the chord line of the airfoil section at 75 percent of span. This chord line is nominally in the plane of rotation during operation in winds of below-rated speed. All loads were measured in the root areas of the rotor blades, at radial distances between 5 and 10 percent of the blade span.

As shown by the straight lines fitted to the test data, cyclic loads were found to have log-normal probability distributions within each test series. The slopes of the curve-fit lines are proportional to the log-standard deviations of the data. Steeper slopes may be attributed to larger variations in wind speed, wind shear, and turbulence during the test series.

Table V summarizes the significant results of this experimental study of blade bending loads. In addition to information on test series duration and mean wind speed, cyclic flatwise and cyclic chordwise bending loads are listed for two percentiles of interest: 50 and 99.9. The 50th percentile load is useful for calibrating theoretical load prediction methods which may not include turbulent winds and operating transients (ref. 15). However, the value of the 50th percentile load for purposes of fatigue life analysis is small because fatigue damage cannot be tolerated at this percentile load in a long-life design. Of more use in life prediction is the 99.9th percentile load. A design fatigue life of 10^6 cycles or more is often required at this load level. Operating load limits for several of the rotor configurations tested in this study were set at predicted 99.9th percentile levels.

The cyclic load data in Table V have been normalized to remove differences in scale, in order to derive general load factors useful for design. A convenient reference for the flatwise load components was found to be the difference between the theoretical steady aerodynamic flatwise bending load at rated wind speed and that at the zero-power (cut-in) wind speed. The reference for chordwise loads was the gravity bending moment measured with the blade horizontal. All reference loads were determined for the radial stations at which the cyclic loads were measured. Load factors were calculated by dividing test loads by the reference loads for the test series.

Variations in flatwise cyclic load factors among the six test series were relatively small, considering the wide variation in rotor

configurations. This tends to verify the assumption that the selected reference load contains the key parameters governing cyclic flatwise blade loading. Flatwise load factors were smallest for test series 1.2 which had the lowest mean wind speed and was conducted at a location with low terrain roughness (Table II). Low terrain roughness usually produces low average wind turbulence. Larger flatwise load factors generally correlated with higher wind speeds and locations with rougher terrain. Averaging the flatwise load test results for the six series gives factors of 0.24 and 0.73 for the 50th and 99.9th percentile cyclic loads, respectively.

Chordwise cyclic load factors averaged 1.11 and 1.46 for the 50th and 99.9th percentile loads, respectively. While it is convenient for design purposes to reference chordwise loads to the dominant gravity load, the components of these load factors in excess of 1.00 have been found to correlate with flatwise cyclic bending, rather than with blade mass properties (ref. 15). Again, variations in chordwise load factors were small for each percentile, although the actual chordwise cyclic loads varied by more than an order of magnitude.

In summary, blade cyclic load spectra for both flatwise and chordwise bending can be estimated for first-generation, horizontal-axis wind turbine blades by applying the load factors and reference loads given in Table V.

CONCLUSIONS

This study has provided a set of test data on the power conversion performance and dynamic blade loading typical of first-generation, horizontal-axis wind turbine generators. The following conclusions are drawn from analysis of these test data:

1. The mean power conversion performance of four test rotor configurations equaled or exceeded system efficiencies as predicted by means of the PROP-L2 computer program.

2. During 64 hours of automatic operation in primarily below-rated winds, the composite system efficiency of the four rotor configurations was 0.34, which compares favorably with a theoretical efficiency of 0.31 for the measured wind conditions.

3. The proposed energy method for analyzing performance test data provided a practical solution to problems presented by wind turbulence and time-varying test data. Results were found to be repeatable for a variety of test rotors and test installations.

4. Blade cyclic load spectra exhibited log-normal distributions in all cases studied.

5. Load factors and reference loads have been derived with which blade fatigue loads can be estimated for design purposes.

UNIT CONVERSION FACTORS

1 m	= 3.28 ft	1 rad/s	= 9.55 rpm
1 m^2	= 10.76 ft^2	1 kN-m	= 738 lb-ft
1 m/s	= 2.24 mph	1 kg/m^3	= 0.00197 $slug/ft^3$

REFERENCES

1. Thomas, R. L. and Robbins, W. H.: Large Wind Turbine Projects. Proc. Fourth Biennial Conf. and Workshop on Wind Energy Conversion Sys., DOE Publ. CONF-791097, 1979, pp. 75-98.

2. Spera, D. A.: Design Evolution of Large Wind Turbine Generators. Large Wind Turbine Design Characteristics and R&D Requirements, DOE Publ. CONF-7904111, NASA CP-2106, 1979, pp. 25-33.

3. Spera, D. A.; Janetzke, D. C.; and Richards, T. R.: Dynamic Blade Loading in the ERDA/NASA 100 kW and 200 kW Wind Turbines. ERDA/NASA/1004-77/2, NASA TM-73711, 1977.

4. Richards, T. R. and Neustadter, H. E.: DOE/NASA Mod-0A Wind Turbine Performance. DOE/NASA/1004-78/13, NASA TM-78916, 1978.

5. Linscott, B. S. and Shaltens, R. K.: Blade Design and Operating Experience on the Mod-0A 200 kW Wind Turbine at Clayton, New Mexico. Large Wind Turbine Design Characteristics and R&D Requirements, DOE Publ. CONF-7904111, NASA CP-2106, 1979, pp. 225-238.

6. Donham, R. E.: Evaluation of an Operating Mod-0A 200 kW Wind Turbine Blade. Large Wind Turbine Design Characteristics and R&D Requirements, DOE Publ. CONF-7904111, NASA CP-2106, 1979, pp. 239-265.

7. Spera, D. A.; Viterna, L. A.; Richards, T. R.; and Neustadter, H. E.: Preliminary Analysis of Performance and Loads Data from the 2-Megawatt Mod-1 Wind Turbine Generator. Proc. Fourth Biennial Conf. and Workshop on Wind Energy Conversion Sys., DOE Publ. CONF-791097, pp. 99-117, NASA TM-81408, 1979.

8. Spera, D. A.: Calculation of Guaranteed Mean Power from Wind Turbine Generators. Wind Turbine Dynamics, DOE Publ. CONF-810226, NASA CP-2185, 1981, pp. 139-150.

9. Andersen, T. S., et al: Mod-0A 200 kW Wind Turbine Generator Design and Analysis Report. DOE/NASA/0163-2, NASA CR-165128, 1980.

10. Neustadter, H. E. and Spera, D. A.: Applications of the DOE/NASA Wind Turbine Engineering Information System. Wind Turbine Dynamics, DOE Publ. CONF-810226, NASA CP-2185, 1981, pp. 113-120.

11. Wilson, R. E.; Lissaman, P. B. S.; and Walker, S. N.: Aerodynamic Performance of Wind Turbines. ERDA/NSF/04014-76/1, 1976.

12. Viterna, L. A. and Corrigan, R. D.: Fixed Pitch Rotor Performance of Large Horizontal-Axis Wind Turbines. DOE/NASA Workshop on Large, Horizontal-Axis Wind Turbines, July 1981.

13. Jacobs, E. M. and Abbott, I. H.: The NACA Variable-Density Wind Tunnel. NACA TR 416, 1932.

14. Akins, R. E.: Performance Evaluation of Wind Energy Conversion Systems Using the Method of Bins--Current Status. Sandia Labs., SAND-77-1375, 1978.

15. Spera, D. A.: Comparison of Computer Codes for Calculating Dynamic Loads in Wind Turbines. DOE/NASA/1028-78/16, NASA TM-73773, 1977.

TABLE I

AIRFOIL GEOMETRY OF WIND TURBINE ROTOR CONFIGURATIONS

Spanwise coordinate		Chord	Thickness to chord ratio	Twist (towards feather)	Skin material
m	percent	m		deg	
(a) Configuration 1 (NACA 23000 series airfoil coned 7 deg)					
1.22	6	1.37	0.440	31.7	Aluminum
2.86	15	1.37	0.372	21.7	Aluminum
4.76	25	1.37	0.291	14.0	Aluminum
5.72	30	1.31	0.250	11.3	Aluminum
9.53	50	1.06	0.212	4.0	Aluminum
14.29	75	0.76	0.166	0	Aluminum
19.05	100	0.46	0.120	-2.0	Aluminum
(b) Configuration 2 (NACA 23000 series airfoil coned 7 deg)					
4.27	22	1.58	0.298	4.2	Wood
14.29	75	0.94	0.156	0	Wood
19.05	100	0.64	0.088	-2.0	Wood
(c) Configuration 3R (NACA 23000 series airfoil coned 7 deg)					
4.27	30	1.52	0.310	0	Wood
8.18	58	1.52	0.240	0	Wood
10.57	75	1.36	0.240	0	Wood
12.47	89	1.24	0.240	0	Fiberglass
13.51	96	1.17	0.217	0	Fiberglass
14.10	100	0	0	0	Fiberglass
Semi-circular tips, beveled both sides, from 13.51 m to 14.10 m					
(d) Configuration 4 (NACA 4400 series airfoil coned 9 deg)					
3.07	10	3.66	0.333	8	Steel
23.05	75	1.64	0.165	0	Steel
30.73	100	0.86	0.100	-3	Steel

TABLE II

WIND TURBINE ROTOR TEST SERIES AND INSTALLATIONS

Rotor config.	Test series no.	Turbine rotor data			Test installation data				
		Shaft speed rad/s	Blade tip speed m/s	Swept area m^2	Wind energy system	Rated power kW	Location	Hub elev. m	Relative terrain roughness
1	1.1	4.3	81	1123	Mod-0A	200	Clayton, NM	1566	medium
	1.2	3.3	63	1123	Mod-0A	150	Culebra, PR	110	low
2	2.1	4.3	81	1123	Mod-0A	200	Kahuku, HI	137	low
	2.2	3.3	63	1123	Mod-0A	150	Block Is., RI	44	high
3R	3.1R	4.3	60	615	Mod-0A	200	Clayton, NM	1566	medium
4	4.1	3.7	111	2894	Mod-1	2000	Boone, NC	1387	high

TABLE III

SUMMARY OF POWER CONVERSION PERFORMANCE OF FOUR DOE/NASA HORIZONTAL-AXIS WIND TURBINES

Test series no.	Test period	Free-stream wind input measured at hub elevation			Mean output power flux at generator		Mean power conversion efficiency	
		Mean wind speed	Mean tip speed ratio	Mean input power flux	Theory [a]	Test	Theory [a]	Test
	hr	m/s		W/m^2	W/m^2	W/m^2		
1.1	11	7.7	10.5	270	89	90	0.33	0.33
2.1	20	8.2	9.9	381	112	111	0.29	0.29
3.1R[b]	22	9.2	6.5	537	141	172	0.26	0.32
4.1	11	10.2	10.9	584	238	250	0.41	0.43
Data set	64	8.8	9.0	450	140	152	0.31	0.34

[a] PROP-L2 computer program, with square-tip loss model
[b] Semi-circular tips on blades; all other blades have square tips

TABLE IV

DEVIATION OF TEST OUTPUT POWER FLUX FROM THEORY,
FOR FOUR DOE/NASA HORIZONTAL-AXIS WIND TURBINES

Test series no.	No. of samples	Mean deviation of samples		Standard deviation of samples		Lower bound on mean deviation (0.999 conf.)	
		W/m^2	% of rated	W/m^2	% of rated	W/m^2	% of rated
(a) Blades with square tips							
1.1	68	1	0.6	11	6.2	-3	-1.7
2.1	119	-1	-0.6	9	5.1	-3	-1.7
4.1	65	12	1.7	39	5.6	-3	-0.4
Data set	252	3	0.3	7	5.5	-3	-1.2
(b) Blades with semi-circular tips (theory for square tips)							
3.1R	131	31	9.5	19	5.8	26	8.0

TABLE V

SUMMARY OF BLADE CYCLIC LOAD TEST DATA
FROM SIX DOE/NASA HORIZONTAL-AXIS WIND TURBINES

Test series	Test period	Mean wind speed	Flatwise cyclic bending loads [a]			Chordwise cyclic bending loads [a]		
			Ref. load [b]	Load factor, by percentile		Ref. load [c]	Load factor, by percentile	
	10^3 rotor revs.	m/s	kN-m	50	99.9	kN-m	50	99.9
1.1	102	9.3	134	0.22	0.85	61.6	1.10	1.48
1.2	86	6.1	118	0.17	0.53	61.6	1.04	1.36
2.1	126	8.8	152	0.24	0.74	68.9	1.12	1.51
2.2	77	6.6	134	0.31	0.75	56.5	1.15	1.58
3.1	126	7.1	108	0.22	0.67	70.5	1.13	1.39
4.1	40	8.8	1177	0.44	0.97	739.	1.08	1.50
Data set	557	7.7	NA	0.24	0.73	NA	1.11	1.46

[a] 0.5 (max load - min load) per rotor revolution, measured at 5% to 10% of span
[b] Steady aerodynamic bending moment change from zero power to rated (PROP-L2 program)
[c] Gravity bending moment, blade horizontal (measured)

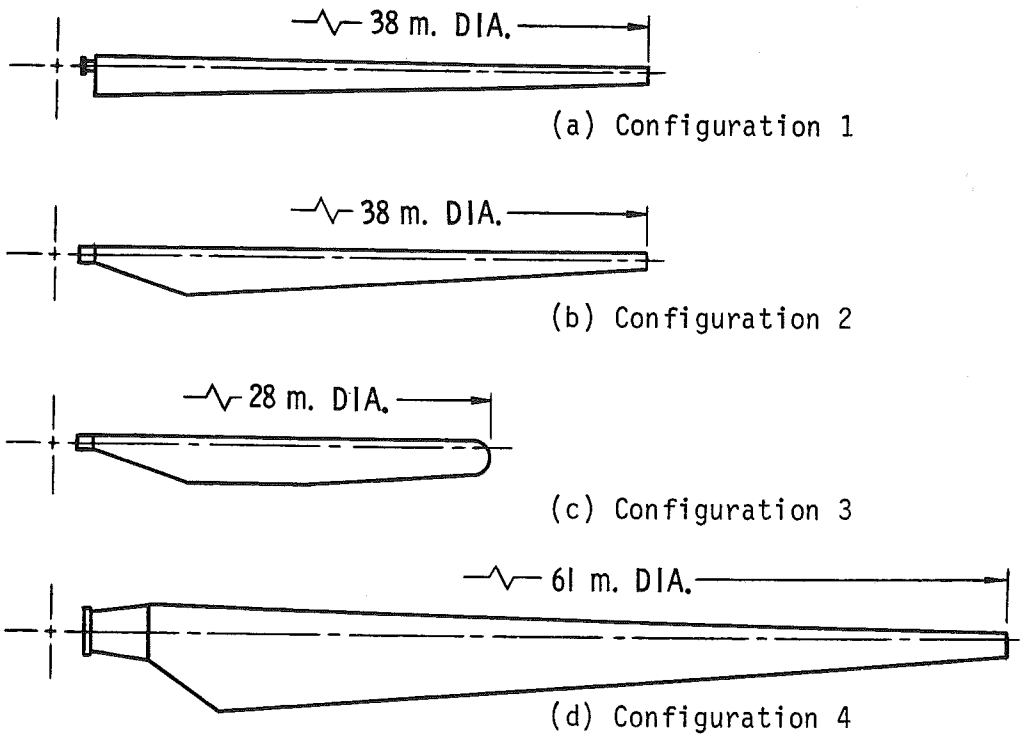

Figure 1. -- Planforms of wind turbine blades tested for power conversion performance and structural loads.

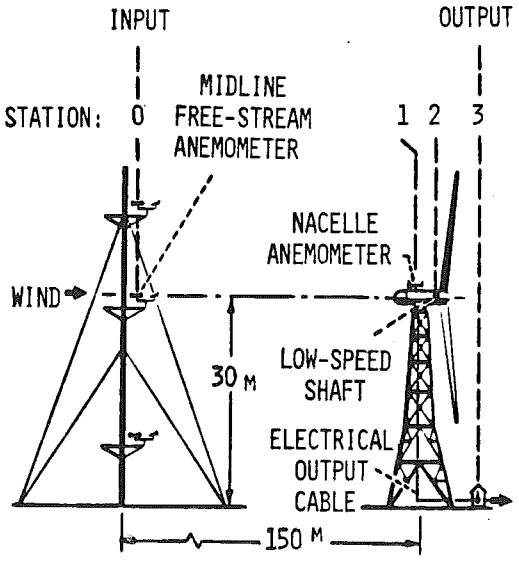

Figure 2. -- Typical performance test installation, showing the Mod-0A 200 kW wind turbine generator, the anemometer tower, and measurement stations at Clayton, New Mexico

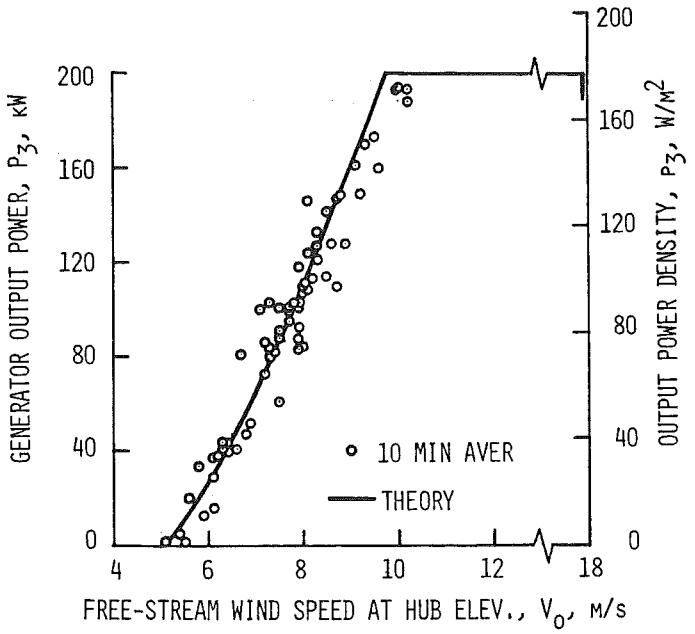

(a) Output power (air density = 1.05 kg/m^3)

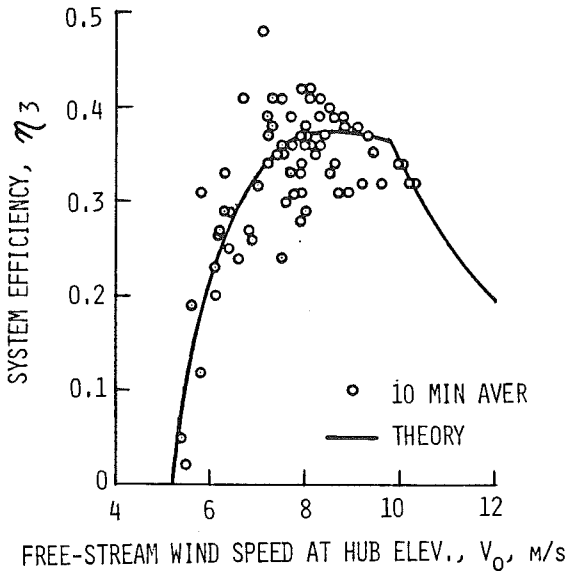

(b) System efficiency

Figure 3. -- Test series 1.1 power conversion performance, compared with theoretical performance (Mod-0A aluminum blades at Clayton, New Mexico).

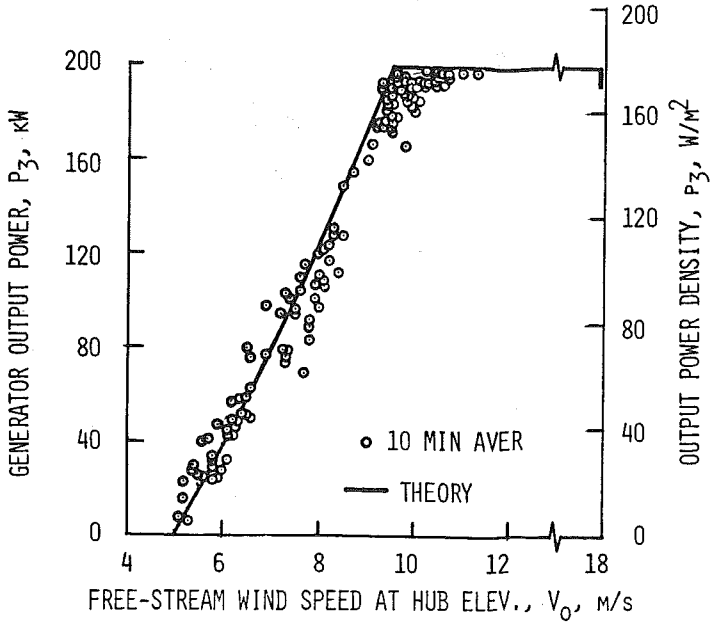

(a) Output power (air density = 1.21 kg/m^3)

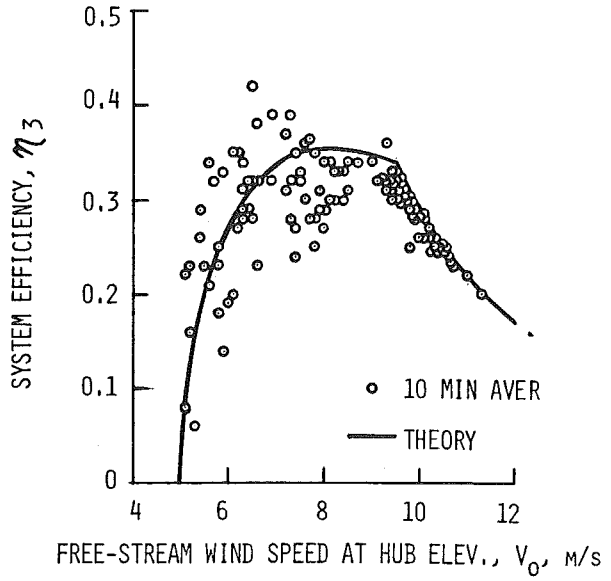

(b) System efficiency

Figure 4. -- Test series 2.1 power conversion performance, compared with theoretical performance (Mod-0A wood blades at Kahuku, Hawaii).

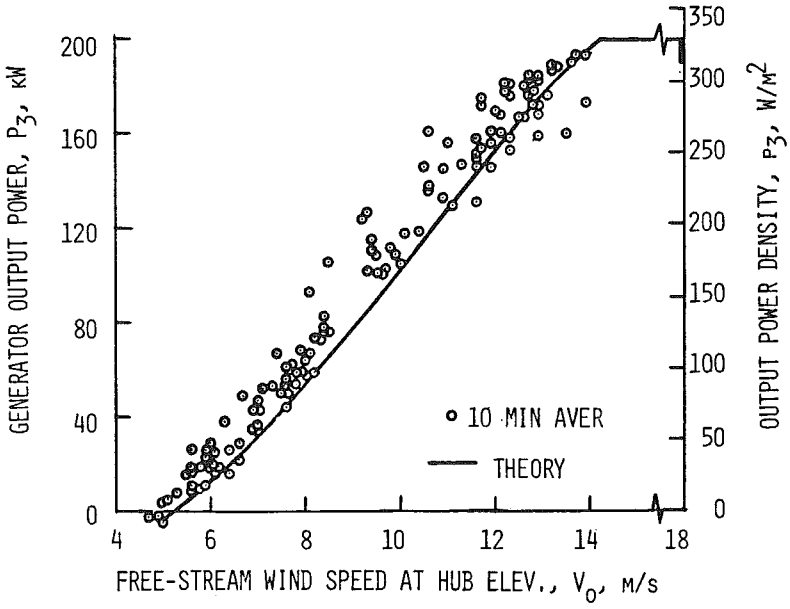

(a) Output power (air density = 1.05 kg/m^3)

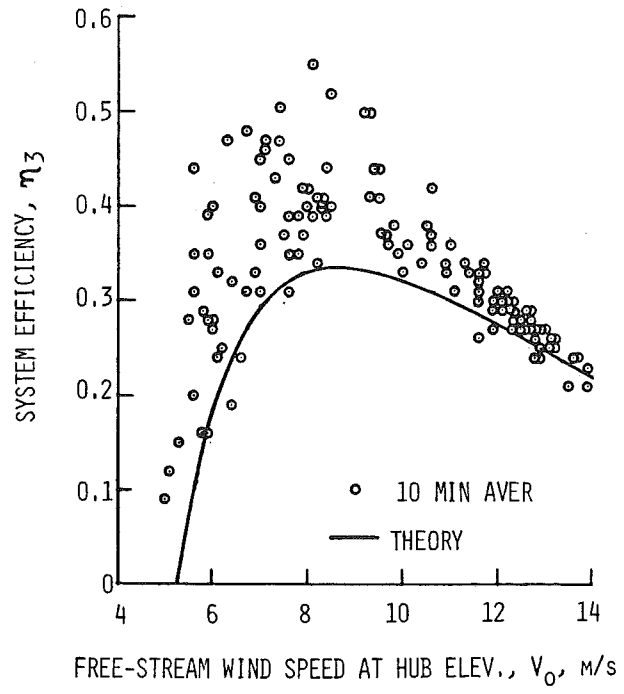

(b) System efficiency

Figure 5. -- Test series 3.1R power conversion performance, compared with theoretical performance (Mod-0A wood/fiberglass blades with semi-circular tips at Clayton, New Mexico).

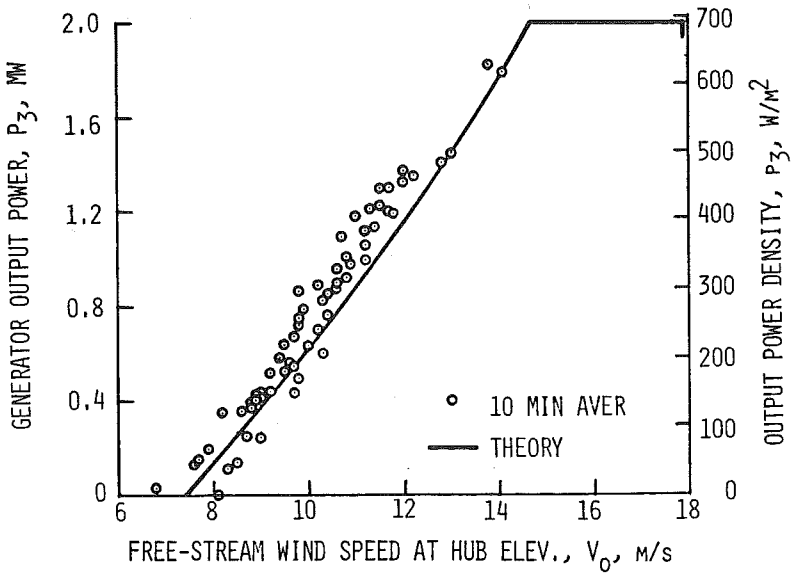

(a) Output power (air density = 1.07 kg/m^3)

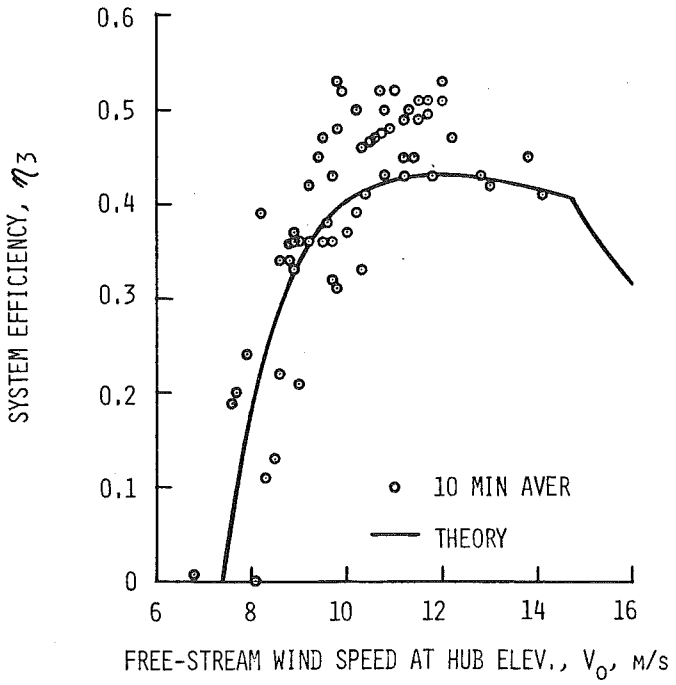

(b) System efficiency

Figure 6. -- Test series 4.1 power conversion performance compared with theoretical performance (Mod-1 steel blades at Boone, North Carolina).

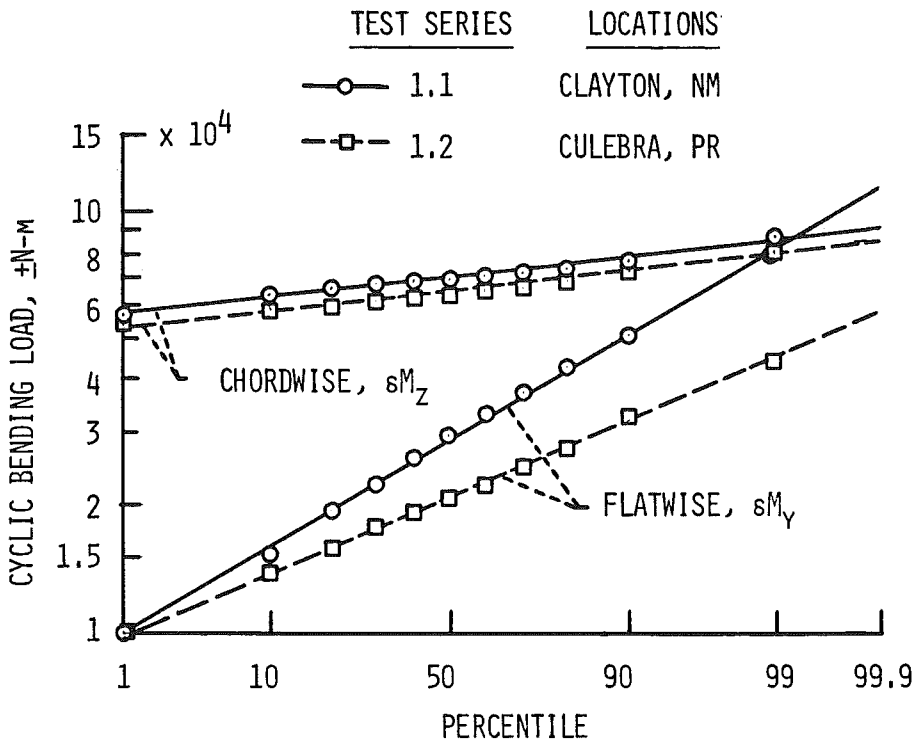

(a) Mod-OA aluminum blades (at 5% span)

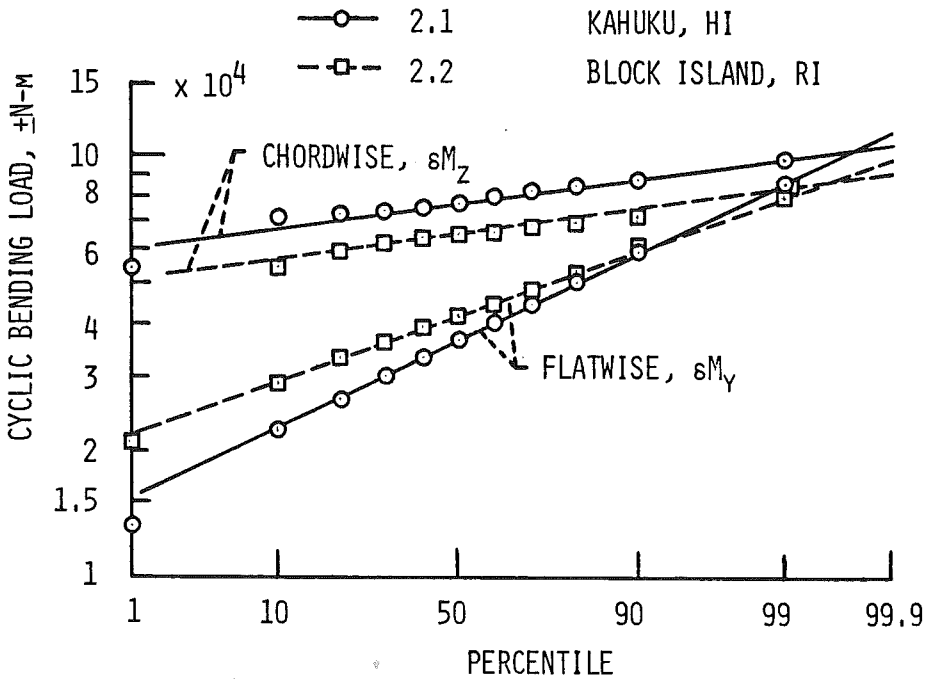

(b) Mod-OA wood blades (at 5% span)

Figure 7. - Probability distributions of blade cyclic bending moments, with log-normal distribution curve-fits.

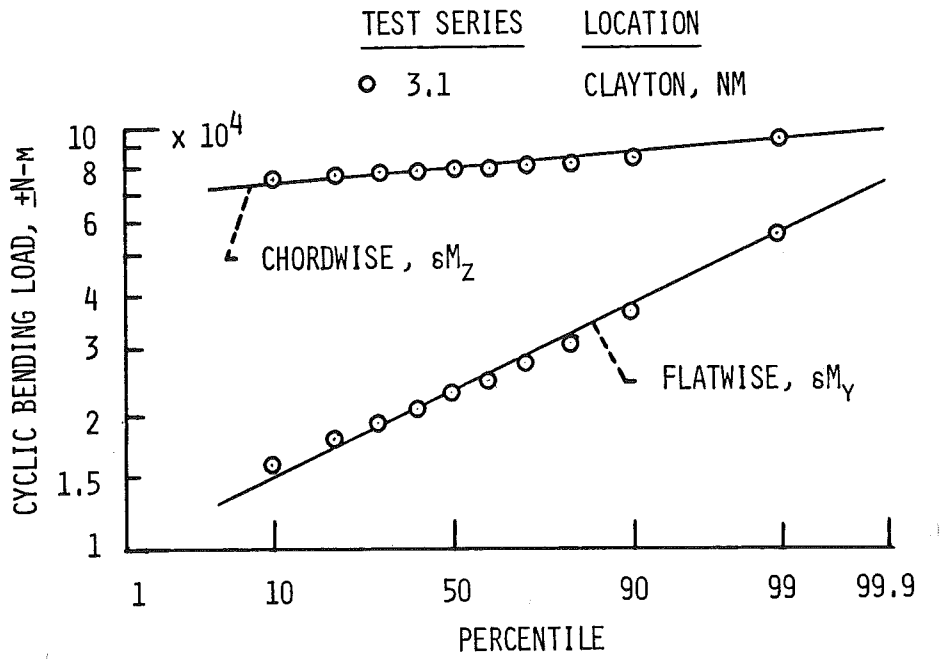

(c) Mod-OA wood/fiberglass blades (at 7% span)

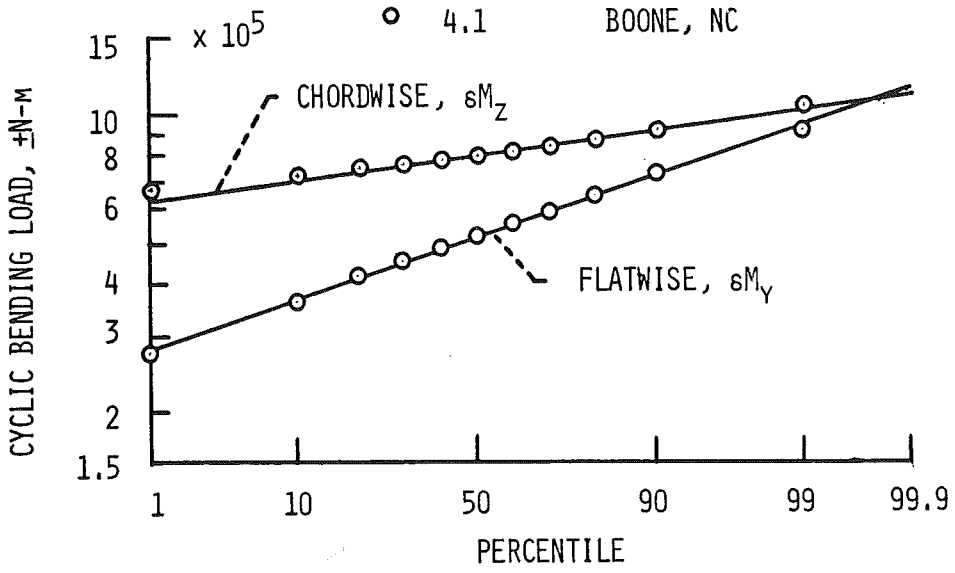

(d) Mod-1 steel blades (at 10% span)

Figure 7 (Concluded). - Probability distributions of blade cyclic bending moments, with log-normal curve-fits.